Journal of Biomolecular NMR (2006) 36:251–257
DOI 10.1007/s10858-006-9089-7

Article

Sensitivity improvement for correlations involving arginine side-chain Nε/Hε resonances in multi-dimensional NMR experiments using broadband ^{15}N 180° pulses

Junji Iwahara & G. Marius Clore*
Laboratory of Chemical Physics, Building 5, National Institute of Diabetes and Digestive and Kidney Disease, National Institutes of Health, Bethesda, MD 20892-0520, USA

Received 11 July 2006; Accepted 14 September 2006

Key words: arginine guanidino group, broadband ^{15}N 180 pulse, off-resonance, pulse imperfection, sensitivity improvement

Abstract

Due to practical limitations in available ^{15}N rf field strength, imperfections in ^{15}N 180° pulses arising from off-resonance effects can result in significant sensitivity loss, even if the chemical shift offset is relatively small. Indeed, in multi-dimensional NMR experiments optimized for protein backbone amide groups, cross-peaks arising from the Arg guanidino ^{15}Nε (~85 ppm) are highly attenuated by the presence of multiple INEPT transfer steps. To improve the sensitivity for correlations involving Arg Nε–Hε groups, we have incorporated ^{15}N broadband 180° pulses into 3D ^{15}N-separated NOE-HSQC and HNCACB experiments. Two ^{15}N-WURST pulses incorporated at the INEPT transfer steps of the 3D ^{15}N-separated NOE-HSQC pulse sequence resulted in a ~1.5-fold increase in sensitivity for the Arg Nε–Hε signals at 800 MHz. For the 3D HNCACB experiment, five ^{15}N Abramovich-Vega pulses were incorporated for broadband inversion and refocusing, and the sensitivity of Arg^{1}Hε-^{15}Nε-^{13}Cγ/^{13}Cδ correlation peaks was enhanced by a factor of ~1.7 at 500 MHz. These experiments eliminate the necessity for additional experiments to assign Arg ^{1}Hε and ^{15}Nε resonances. In addition, the increased sensitivity afforded for the detection of NOE cross-peaks involving correlations with the ^{15}Nε/^{1}Hε of Arg in 3D ^{15}N-separated NOE experiments should prove to be very useful for structural analysis of interactions involving Arg side-chains.

Introduction

Guanidino groups of arginine (Arg) side-chains often play a key role in protein function, particularly with regard to ligand binding via specific electrostatic interactions. The guanidino NH_2 groups are difficult to observe because of rapid exchange with water as well as exchange between equivalent protons through Cζ–Nη and Cζ–Nε bond rotations (Yamazaki et al., 1995; Nieto et al., 1997). The Nε–Hε group, however, is relatively easy to detect by NMR. Because the spin-systems involving the Nε–Hε group are similar to those for backbone amide groups, arginine Nε–Hε groups are observable in many multi-dimensional NMR experiments employed for backbone amide groups (e.g., 3D ^{15}N-separated NOE-HSQC, Talluri and Wagner, 1996; and 3D HNCACB,

*To whom correspondence should be addressed. E-mail: mariusc@intra.niddk.nih.gov

Wittekind and Mueller, 1993, Muhandiram and Kay, 1994). Conventionally, rectangular ^{15}N pulses are applied in heteronuclear NMR experiments. Available rf field strengths for ^{15}N, however, are relatively weak in practice due to both the low gyromagnetic ratio of ^{15}N and instrumental design

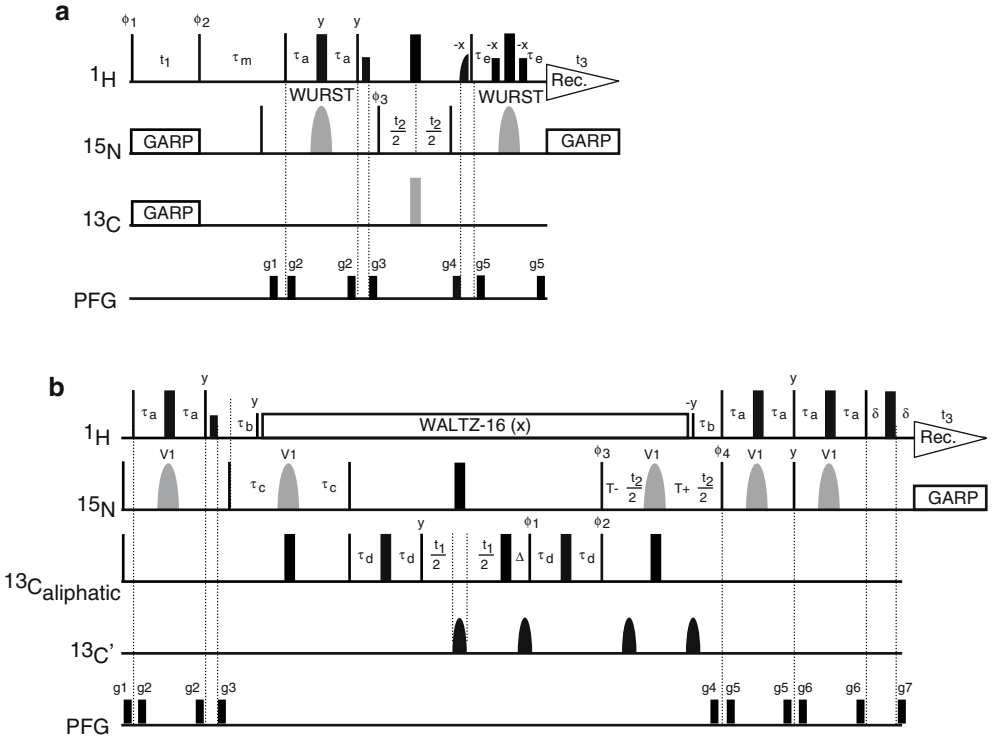

Figure 1. Pulse sequences with broadband ^{15}N 180° pulses designed to improve sensitivity for the observation of cross-peaks involving correlations with Arg side-chain Nε–Hε groups. (a) 3D water-flip-back ^{15}N-separated NOE-HSQC with ^{15}N WURST 180° pulses. The experiment was carried out at a ^{1}H-frequency of 800 MHz. Narrow and wide bars indicate rectangular 90° and 180° pulses, respectively. Phases are along x unless indicated otherwise. Short wide bars represent soft rectangular 90° pulses selective to the $^{1}H_2O$ resonance (1.4 ms). A half-bell shape for ^{1}H represents a half-Gaussian 90° pulse selective for the water resonance (2.0 ms). The ^{15}N carrier position was set to 116 ppm. ^{15}N rectangular 90° pulses were applied with $\gamma B_1/2\pi = 5.6$ kHz. The ^{15}N WURST-20 pulses (represented by grey bell-shapes) were applied with a length of 1.25 ms, an adiabatic sweep-width of 36 kHz, and maximum $\gamma B_1/2\pi$ of 3.9 kHz. Delays are as follows: $\tau_a = 2.25$ ms and $\tau_e = \tau_a$–(length of water-selective pulse). During the NOE mixing time τ_m, the water magnetization immediately returns back to $+z$ through radiation damping (Talluri and Wagner, 1996) and is kept there through the application of a water-flip-back pulse (Grzesiek and Bax, 1993). ^{15}N-GARP decoupling was applied during t_1 and t_3 evolution periods with $\gamma B_1/2\pi = 1.3$ kHz. ^{13}C-decoupling during the ^{15}N-evolution period was carried out with two consecutive 180° pulses for $^{13}C\alpha$ and $^{13}C'$ ($\gamma B_1/2\pi = 14$ kHz). Phase cycling: $\phi_1 = (x, -x)$; $\phi_2 = x + 45°$; $\phi_3 = (x, x, -x, -x)$; receiver $= (x, -x, -x, x)$. The 45° phase-shift for ϕ_2 is for optimal balancing of water-magnetization of real and imaginary scans during the t_1 evolution period. Quadrature detection using States-TPPI for ^{1}H and ^{15}N dimensions was achieved by incrementing the phases of ϕ_1 and ϕ_3, respectively. Pulse field gradients were applied along z and the magnitudes were adjusted to minimize the H_2O signal. (b) 3D HNCACB experiment with ^{15}N V1 180° pulses. The experiment was carried out at a ^{1}H-frequency of 500 MHz. ^{15}N V1 180° pulses were applied with a length of 1.03 ms and a maximum $\gamma B_1/2\pi$ value of 5.2 kHz. The other hard ^{15}N pulses were applied with a rf field strength of 5.2 kHz. A rectangular ^{15}N 180° pulse was used for ^{15}N-decoupling during the t_1 evolution period since a V1 pulse at this position would make the overall duration for ^{13}C transverse magnetization longer. Carrier positions for ^{15}N, $^{13}C_{aliphatic}$, and $^{13}C'$ were set to 116 ppm, 43 ppm, and 177 ppm, respectively. For inversion of carbonyl and arginine Cζ (~159 ppm) nuclei, sinc 180° pulses (240 μs) were applied. To maintain ^{15}N in-phase magnetization, a ^{1}H-WALTZ-16 composite pulse, sandwiched by additional hard ^{1}H 90° pulses to minimize saturation and dephasing of water magnetization (Kay et al., 1994), was applied with a rf field strength of 3.3 kHz. Delays are as follows: $\tau_a = 2.3$ ms; $\tau_b = 5.5$ ms; $\tau_c = 12.4$ ms; $\tau_d = 3.5$ ms; $T = 14.8$ ms; $\Delta =$ (length of $^{13}C'$ sinc 180 pulse) + (initial delay for t_1); $\delta = 375$ μs. Phase cycling: $\phi_1 = (-y, -y, y, y)$; $\phi_2 = (x, x, -x, -x)$; $\phi_3 = (x, -x)$; $\phi_4 = x$; receiver $= (x, -x, -x, x)$. Quadrature detection in the ^{13}C dimension was achieved by simultaneous phase decrementation of ϕ_1 and ϕ_2 using States-TPPI. The phase ϕ_4 and the sign of gradient g4 were inverted for sensitivity-enhanced quadrature detection in the ^{15}N dimension (Muhandiram and Kay, 1994). Pulse field gradients along z for coherence selection were as follows: g4 (2.705 ms, 21 G/cm) and g7 (275 μs, 21 G/cm). The other gradients were adjusted to minimize the solvent signal.

(especially for cryogenic probes), Thus, although the Arg ^{15}Nε resonances (~85 ppm) are not that far upfield from backbone ^{15}N resonances (100–135 ppm), the performance of rectangular 180° pulses applied at ca 120 ppm with a typical rf field strength is imperfect for Arg ^{15}Nε nuclei, resulting in significant loss in sensitivity. This effect is serious for experiments incorporating multiple ^{15}N rectangular 180° pulses, particularly at high magnetic fields.

Here, we demonstrate that incorporation of ^{15}N broadband shaped 180° pulses can significantly enhance the sensitivity of cross-peaks involving the Arg Nε–Hε group in 3D ^{15}N-separated NOE-HSQC and HNCACB experiments, without perturbing the sensitivity of correlations involving the backbone amide groups. Since these experiments are commonly used for analysis of the backbone amides, the technique described here eliminates the necessity for additional experiments to optimally observe correlations involve the Arg Nε–Hε group. The present work provides a useful tool in the NMR characterization of protein–DNA (and RNA) complexes, in which Arg residues are invariably involved in crucial interactions at molecular interfaces.

Materials and methods

NMR samples

The complex between U-[^{13}C-,^{15}N]-labeled HOXD9 homeodomain and a 24-bp DNA oligonucleotide (comprising a duplex of 5′-CACCTCTCTAATGGCTCACACCTG-3′ and its complementary strand) were prepared as described (Iwahara and Clore, 2006a, b). For this study, 0.5 mM complex was dissolved in a buffer containing 10 mM sodium phosphate (pH 5.8), 20 mM NaCl and 7% D_2O.

NMR spectroscopy

Measurements of 3D ^{15}N-separated NOE-HSQC spectra on the U-[^{13}C-,^{15}N]-labeled HOXD9 homeodomain bound to the 24-bp DNAduplex were carried out on a Bruker DRX-800 spectrometer. 3D HNCACB spectra were recorded using a Bruker DMX-500 spectrometer. Both spectrometers were equipped with cryogenic probes and all spectra were recorded at 35 °C. Wave files for WURST-20 (Kupce and Freeman, 1995) and Abramovich–Vega (Abramovich and Vega, 1993) pulses were created with the 'shapeTool' utility in the xwinnmr software package. Hereafter, we refer to the latter pulse as a "V1" pulse according to previous literature (Ogura et al., 1996; Zweckstetter and Holak, 1999). In 'shapeTool', the "IVega" shape was specified for a V1 pulse. Other details are described in the caption to Figure 1.

Results and discussion

Imperfections in ^{15}N rectangular pulses due to off-resonance effects

First, we consider the off-resonance effect for rectangular pulses applied with an rf field strength of 5.5 kHz, which corresponds to typical ^{15}N hard pulses used experimentally (90° pulse width of 45–50 μs). Application of a rectangular pulse (with length t_p and x-phase) transforms the z-magnetization into (van de Ven, 1995):

$$M_x = \frac{M_0\omega_1\Omega}{\omega_e^2}\left\{1 - \cos(\omega_e t_p)\right\} \quad (1)$$

$$M_y = \frac{M_0\omega_1}{\omega_e}\sin(\omega_e t_p) \quad (2)$$

$$M_z = \frac{M_0}{\omega_e^2}\left\{\Omega^2 + \omega_1^2\cos(\omega_e t_p)\right\} \quad (3)$$

where Ω is the offset, $\omega_1 = \gamma B_1$, and ω_e is the effective precession frequency given by $\sqrt{\omega_1^2 + \Omega^2}$. If the ^{15}N pulses are applied at 116 ppm, Ω for an Arg ^{15}Nε at 85 ppm is 2.5 kHz at a magnetic field corresponding to a ^{1}H frequency of 800 MHz. In this case, the resultant longitudinal magnetization obtained by application of a 180° pulse is calculated to be $M_z = -0.618\ M_0$ and the transverse magnetization obtained by a 90° pulse is $\sqrt{M_x^2 + M_y^2} = 0.999\ M_0$. Because of the imperfection of the 180° pulse, the efficiency of an INEPT scheme involving ^{15}N is scaled down to 81% for the Arg Nε. At a ^{1}H frequency of 800 MHz, signals involving the ^{15}Nε–^{1}Hε group are scaled

down to 65% and 35% for pulse sequences involving two and five INEPT schemes, respectively. The corresponding numbers at 500 MHz are 85% and 66%, respectively. Hence, incorporation of broadband ^{15}N shaped 180° pulses instead of rectangular 180° pulses should significantly improve the sensitivity for arginine Nε–Hε signals in multi-dimensional NMR experiments used for protein backbone amide groups.

3D ^{15}N-separated NOE-HSQC with ^{15}N WURST pulses

To improve the sensitivity for NOE cross peaks involving the Arg Nε–Hε group, we replaced ^{15}N rectangular 180° pulses in a 3D ^{15}N-separated NOE-HSQC pulse sequence by broadband WURST pulses (Kupce and Freeman, 1995) as shown in Figure 1a. Since the bandwidth used for uniform inversion by the WURST pulse was ±12 kHz, the longitudinal magnetizations of Arg ^{15}Nε nuclei are fully inverted by the INEPT schemes. Another advantage is that WURST pulses are robust and less sensitive to rf inhomogenity and mis-calibration (Kupce, 2001). The 3D ^{15}N-separated NOE-HSQC experiment with ^{15}N WURST pulses was compared to that with ^{15}N rectangular 180° pulses. Although the use of a WURST pulse could change the net *J*-evolution during the INEPT schemes (Kupce and Freeman, 1997; Zwahlen et al., 1997), efficiencies of the coherence transfers in the present study appeared to be unaffected. Spectra were measured on the complex between the U-[^{13}C,^{15}N]-HOXD9 homeodomain and a 24-bp DNA duplex containing the homeodomain specific target site. Experiments were recorded at 800 MHz under identical conditions with the ^{15}N-carrier position set to 116 ppm and rectangular ^{15}N pulses applied with an rf field strength of 5.6 kHz. As expected from the theoretical considerations described above, incorporation of two ^{15}N WURST pulses in place of the

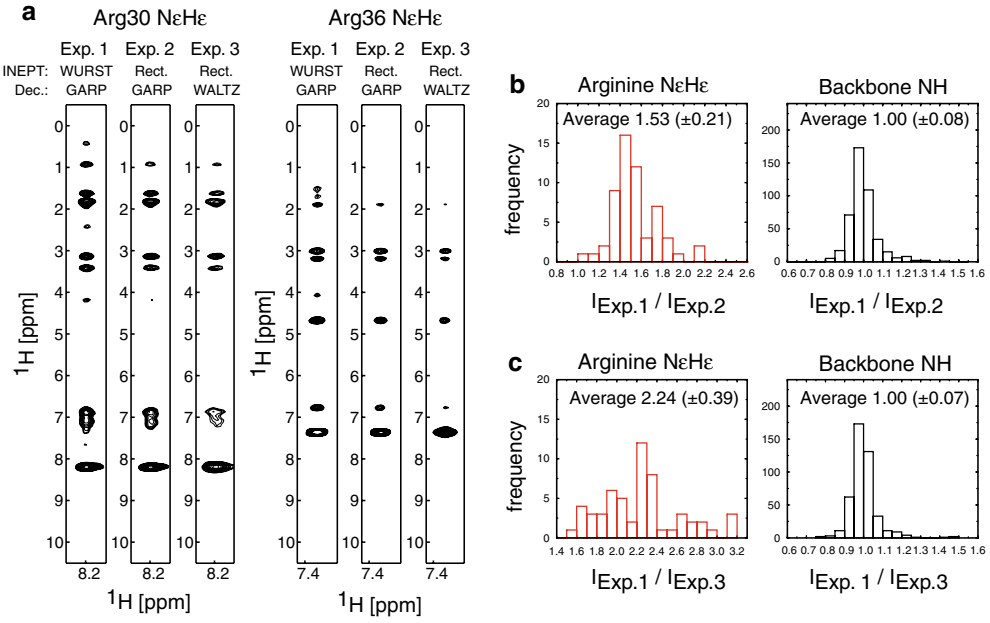

Figure 2. Sensitivity improvement for cross-peaks involving arginine Nε–Hε correlations in a 3D ^{15}N-separated NOE-HSQC spectrum obtained by incorporating ^{15}N WURST 180° pulses (^{1}H-frequency, 800 MHz). Three experiments were compared (panel a): Exp. 1, with ^{15}N WURST 180° pulses and ^{15}N GARP decoupling during acquisition; Exp. 2, with ^{15}N rectangular 180° pulses and ^{15}N GARP decoupling; and Exp. 3, with ^{15}N rectangular 180° pulses and ^{15}N WALTZ-16 decoupling. The rf field strengths for the hard ^{15}N rectangular and composite decoupling pulses were set to 5.6 kHz and 1.3 kHz, respectively. The NOE mixing time τ_m was set to 80 ms. (a) ^{1}H(F_1)–^{1}H(F_3) strips for the Nε–Hε groups of Arg30 (^{15}N, 85.19 ppm) and Arg36 (^{15}N, 83.54 ppm) taken from the 3D spectra recorded using Exp. 1, 2 and 3 (all plotted at the same contour level). (b) Histograms of ratios of signal intensities in Exp. 1 and Exp. 2. Results for arginine Nε–Hε and backbone N–H correlations are shown separately. Since all three experiments were recorded using exactly the same conditions, the noise standard deviations for the three spectra are identical, and the ratios shown here represent the improvement in signal-to-noise (S/N) ratio for individual peaks. (c) Same as panel b, but comparing Exp. 1 with Exp. 3.

rectangular 180° pulses improved the signal-to-noise (S/N) ratio for cross-peaks involving the Nε–Hε Arg groups by a factor of 1.53 ± 0.21 while leaving the S/N ratio for correlations involving the backbone amide groups completely unaltered (Figure 2b). For both experiments, we employed ^{15}N-GARP decoupling (Shaka and Keeler, 1987) with a rf field strength of 1.3 kHz. Although ^{15}N-WALTZ-16 decoupling (Shaka et al., 1983) is more commonly used for the 3D ^{15}N-separated NOE experiments (Marion et al., 1990; Talluri and Wagner, 1996), the signals

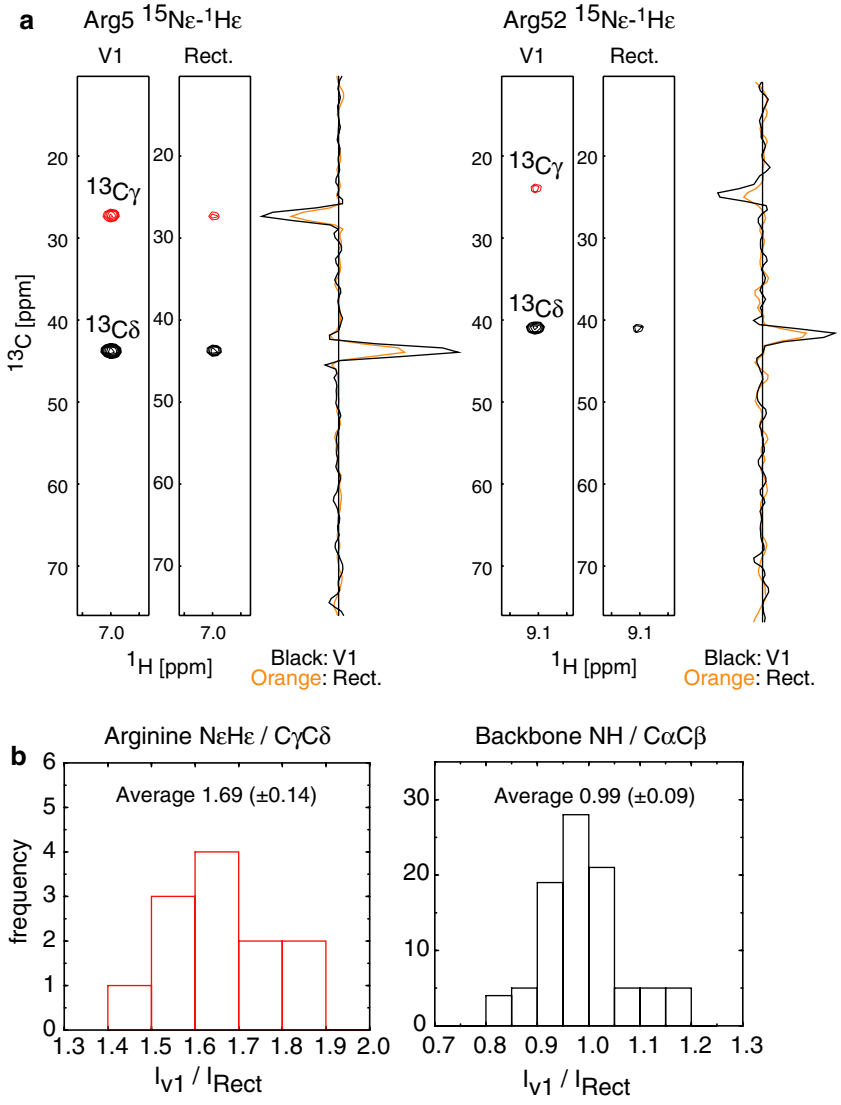

Figure 3. Sensitivity improvement for Arg Nε–Hε signals in a 3D HNCACB spectrum obtained by incorporating ^{15}N V1 180° pulses (^{1}H-frequency, 500 MHz). The experiments with ^{15}N V1 pulses (Figure 1b) and ^{15}N rectangular 180° pulses ($\gamma B_1/2\pi$ = 5.2 kHz) at the corresponding positions are compared. (a) ^{1}H(F_3)–^{13}C(F_1) strips for N–H groups of Arg5 (^{15}N, 84.88 ppm) and Arg52 (^{15}N, 88.09 ppm) taken from the 3D spectra recorded with ^{15}N V1 and rectangular 180° pulses (denoted as V1 and Rect, respectively) and plotted at the same contour level (black, positive contours; red, negative contours). The two ^{13}C resonances are for Arg ^{13}Cγ (negative) and ^{13}Cδ (positive). For each residue, an overlay of 1D slices along the ^{13}C dimension for the two experiments are shown on the right-hand side. (b) Histograms of ratios of signal intensities in the two spectra measured with ^{15}N V1 and rectangular 180° pulses. Results for Arg Nε–Hε and backbone N–H are shown separately. Since the two experiments were recorded using exactly the same conditions, the noise level for the two spectra are identical and the histograms represent the improvement in S/N ratios afforded by the use of ^{15}N V1 pulses.

involving Arg Nε–Hε groups were further weakened when WALTZ-16 was employed. This is because the bandwidth for WALTZ-16 is much narrower than that for GARP and consequently decoupling of the Arg ^{15}Nε is insufficient, even though the corresponding ^{1}Hε signal appears to be a singlet. Compared to a 3D ^{15}N-separated NOE-HSQC with ^{15}N rectangular 180° pulses and WALTZ-16 decoupling, the experiment with ^{15}N WURST 180° pulses and GARP decoupling yielded S/N enhancement of a factor of 2.24 ± 0.39 for Arg Nε–Hε groups (Figure 2c).

3D HNCACB experiment with ^{15}N V1 pulses

We applied a similar strategy for the 3D HNCACB experiment. Although this triple resonance experiment was originally developed for assignment of backbone amide ^{15}N–^{1}H and ^{13}Cα/^{13}Cβ resonances, it is also useful for assignment of Arg ^{15}Nε and ^{1}Hε resonances, via intra-residue correlations between ^{15}Nε–^{1}Hε and ^{13}Cγ/^{13}Cδ since the spin-system for the Arg Nε–Hε is similar to that for a backbone amide. (Note, the chemical shifts for ^{13}Cδ, ^{13}Cγ, and ^{13}Cζ of Arg are ∼43 ppm, ∼27 ppm and ∼159 ppm, respectively, corresponding to ^{13}Cα, ^{13}Cβ and ^{13}C' for backbone amide). Even at low magnetic field, the sensitivity-loss for Arg Nε–Hε due to the ^{15}N off-resonance effect is expected to be significant since five ^{15}N 180° pulses are involved in INEPT transfers in the standard gradient-enhanced HNCACB experiment (Muhandiram and Kay, 1994). For simultaneous detection of backbone amide and Arg Nε–Hε resonances with high sensitivity in a 3D HNCACB experiment, we incorporated five ^{15}N V1 broadband pulses (Abramovich and Vega, 1993) for INEPT transfers instead of rectangular 180° pulses (Figure 1b). A nice feature of the V1 pulse is that it works well for both broadband inversion and refocusing (Ogura et al., 1996), whereas a WURST pulse does not serve as a broadband refocusing pulse on its own. (Note a drawback is that the V1 pulse requires higher power). The ^{15}N V1 pulse we employed exhibits uniform inversion and refocusing over ±3.5 kHz. We recorded the 3D HNCACB spectrum with the broadband ^{15}N pulses and compared the intensities of ^{1}Hε-^{15}Nε-^{13}Cγ/^{13}Cδ cross-peaks to those measured with ^{15}N rectangular 180° pulses. Although the experiments were carried out at a relatively low magnetic field (^{1}H frequency 500 MHz), the incorporation of broadband ^{15}N V1 pulses resulted in a significant improvement in S/N ratio for correlations involving the Arg Nε–Hε (Figure 3). The average S/N enhancement was 1.69 ± 0.14 for ^{1}Hε-^{15}Nε-^{13}Cγ/^{13}Cδ cross peaks, while maintaining the same sensitivity for backbone ^{1}H-^{15}N-^{13}Cα/^{13}Cβ cross-peaks (Figure 3b).

Concluding remarks

In this paper, we have demonstrated that incorporation of ^{15}N broadband shaped 180° pulses results in very significant increases in sensitivity for correlations involving Arg Nε–Hε signals in standard multi-dimensional NMR experiments for proteins. Similar attempts at sensitivity improvement by incorporation of broadband 180° pulses had been made previously for ^{13}C in protein NMR spectroscopy (Hallenga and Lippens, 1995; Ogura et al., 1996; Zweckstetter and Holak, 1999), since the ^{13}C chemical shift distribution is very large. Although the range of ^{15}N chemical shifts for N–H groups in proteins is smaller in units of Hz relative to ^{13}C, the relatively low rf field strengths available for ^{15}N in practice result in large losses in sensitivity for Arg Nε–Hε signals in experiments optimized for backbone amide groups when conventional 180° rectangular ^{15}N pulses are employed. With the improved sensitivity afforded by the incorporation of broadband ^{15}N pulses in the 3D ^{15}N-separated NOE-HSQC and HNCACB experiments described here, signals from Arg Nε–Hε groups can be easily assigned without additional experiments. Further, the observation of NOE cross-peaks to Arg ^{1}Hε protons at higher sensitivity should prove extremely useful for structural analysis of Arg side-chains.

Acknowledgments

This work was supported by funds from the Intramural Program of the NIH, NIDDK and in part by the AIDS Targeted Antiviral program of the Office of the Director of the NIH (to G.M.C.).

References

Abramovich, D. and Vega, S. (1993) *J. Magn. Reson. Ser. A*, **105**, 30–48.

Grzesiek, S. and Bax, A. (1993) *J. Am. Chem. Soc.*, **115**, 12593–12594.

Hallenga, K. and Lippens, G.M. (1995) *J. Biomol. NMR*, **5**, 59–66.
Iwahara, J. and Clore, G.M. (2006a) *J. Am. Chem. Soc.*, **128**, 404–405.
Iwahara, J. and Clore, G.M. (2006b) *Nature*, **440**, 1227–1230.
Kay, L.E., Xu, G.Y. and Yamazaki, T. (1994) *J. Magn. Reson. Ser. A*, **109**, 129–133.
Kupce, E. and Freeman, R. (1995) *J. Magn. Reson. Ser. A*, **115**, 273–276.
Kupce, E. and Freeman, R. (1997) *J. Magn. Reson.*, **127**, 36–48.
Kupce, E. (2001) *Methods Enzymol.*, **338**, 82–111.
Marion, D., Driscoll, P.C., Kay, L.E., Wingfield, P.T., Bax, A., Gronenborn, A.M. and Clore, G.M. (1990) *Biochemistry*, **28**, 6150–6156.
Muhandiram, D.R. and Kay, L.E. (1994) *J. Magn. Reson. Ser. B*, **103**, 203–216.
Nieto, P.M., Birdsall, B., Morgan, W.D., Frenkiel, T.A., Gargaro, A.R. and Feeney, J. (1997) *FEBS Lett.*, **405**, 16–20.
Ogura, K., Terasawa, H. and Inagaki, F. (1996) *J. Magn. Reson. Ser. B*, **112**, 63–68.
Shaka, A.J. and Keeler, J. (1987) *Prog. NMR Spectroscopy*, **19**, 47–129.
Shaka, A.J., Keeler, J. and Freeman, R. (1983) *J. Magn. Reson.*, **52**, 313–340.
Talluri, S. and Wagner, G. (1996) *J. Magn. Reson. Ser. B*, **112**, 200–205.
van de Ven, F.J.M. (1995) *Multidimensional NMR in Liquids: Basic Principles and Experimental Methods*, VCH Publishers, New York.
Wittekind, M. and Mueller, L. (1993) *J. Magn. Reson. Ser. B*, **101**, 201–205.
Yamazaki, T., Pascal, S.M., Singer, A.U., Forman-Kay, J.D. and Kay, L.E. (1995) *J. Am. Chem. Soc.*, **117**, 3556–3564.
Zwahlen, C., Legault, P., Vincent, S.J.F., Greenblatt, J., Konrat, R. and Kay, L.E. (1997) *J. Am. Chem. Soc.*, **119**, 6711–6721.
Zweckstetter, M. and Holak, T.A. (1999) *J. Biomol. NMR*, **15**, 331–334.